research articles Journal of proteome research

Metabolomics Approach for Investigation of Effects of Dengue Virus Infection Using the EA.hy926 Cell Line

Grace Birungi,[†] Sheryl Meijie Chen,[†] Boon Pheng Loy,[‡] Mah Lee Ng,[‡] and Sam Fong Yau Li*[,†]

Department of Chemistry, National University of Singapore, 3 Science Drive 3, Singapore 117543, and Department of Microbiology, Yong Loo Lin School of Medicine, National University Health System, National University of Singapore, 5 Science Drive 2, Singapore 117597

Received July 13, 2010

This paper describes a multiplatform analytical approach combining proton nuclear magnetic resonance (^{1}H NMR) spectroscopy and mass spectrometry (MS), together with pattern recognition tools in a metabolomic study used to investigate the effects of dengue virus infection. The four serotypes of dengue, DEN-1, DEN-2, DEN-3, and DEN-4, were inoculated into the EA.hy926 cell line, which was then incubated for various time intervals. Principal component analysis (PCA) of the ^{1}H NMR and MS data revealed metabolic profile patterns or fingerprint patterns that can be attributed to specific virus serotypes. Distinct effects of infection by each serotype were demonstrated, and these differences were attributed to changes in levels of metabolites (including amino acids, dicarboxylic acids, fatty acids, and organic acids related to the tricarboxylic acid (TCA) cycle). The study demonstrated application of metabolomics to improve understanding of the effect of dengue infection on endothelial cells' metabolome.

Keywords: Dengue • metabolomics • metabolic profiling • EA.hy926 • ^{1}H NMR • MS

1. Introduction

The dengue virus belongs to the *Flaviviridae* family.[1] It has four serotypes: dengue virus 1, 2, 3, and 4 (DEN-1, DEN-2, DEN-3, and DEN-4).[2] All are known to be infectious. In tropical countries, the warm and humid climate is adequate for habitation of *Aedes aegypti* mosquito, a natural host vector for the dengue virus. Therefore, tropical countries are prone to outbreaks of dengue fever (DF), which can develop into more serious cases of dengue hemorrhagic fever (DHF) and dengue hemorrhagic shock syndrome (DSS).[1] This is a public health issue, and it is a threat especially because little is known about the molecular mechanisms underlying infection with dengue.

Previous studies on the effects of dengue virus infection provided genomic[3,4] and proteomic[5] perspectives into understanding the mechanisms of infection, but they have mostly been limited to DEN-2 studies in particular because it is the most common serotype out of the four. A metabolomic approach would add onto this information, and in fact, Kanlaya et al.[5] suggested the need for metabolomic analysis to complement proteomic studies. In this study, metabolomics (or metabonomics) approaches were used to investigate the effects of dengue infection on the EA.hy926 cell line.

EA.hy926 is an endothelial cell line obtained from a hybrid of primary human umbilical vein cells and the thioguanine-resistant clone of A549 (carcinomic epithelial cells from human lungs), and it was used because endothelial cells are susceptible to dengue infection. Furthermore, our study was done in vitro, and the cell line EA.hy926 is a model cell line for this kind of study. Literature reports[5−9] suggest that vascular leakage is an important mechanism in dengue shock syndrome, and due to lack of an appropriate animal model that can precisely simulate dengue virus infection in humans, such studies have mainly been done in vitro using cultivated endothelial cells.

Metabolites were profiled to gain an understanding of how dengue infection alters metabolic pathways in mammals, and differences in the effects of infection caused by different viral serotypes were also investigated. We also attempted to identify potential biomarkers of dengue infection by comparing the metabolic profiles obtained from infected and uninfected cells.

Analytical techniques like high-resolution proton nuclear magnetic resonance (^{1}H NMR) spectroscopy have been used widely to investigate and profile metabolic variations associated with different conditions such as stages of cell growth in human hepatoma cells,[10] onset of epithelial ovarian cancer,[11] and drug-induced toxicity and its effects on fatty acid metabolism.[12]

In our study, ^{1}H NMR spectroscopy was used because it generally requires minimal sample preparation, exhibits high reproducibility, does not destroy the sample, and has relatively short data acquisition times. Furthermore, quantitative measurements of a wide range of compounds can be achieved in a single acquisition, and many metabolites can be analyzed without bias as long as the metabolite has at least a proton. However, ^{1}H NMR spectroscopy has a low sensitivity especially for metabolites present in low concentrations. In this study, we used mass spectroscopy in addition to ^{1}H NMR because it

* Corresponding author. Professor Sam F. Y. Li, National University of Singapore, Department of Chemistry, 3 Science Drive 3, Singapore 117543. Tel: (65)-6516-2681. Facsmile: (65)-6779-1691. E-mail: chmlifys@nus.edu.sg.
† Department of Chemistry.
‡ Department of Microbiology.

10.1021/pr100727m

Published on Web 10/18/2010

offers higher sensitivity compared to ^{1}H NMR spectroscopy. Direct injection mass spectrometry was used in our study. It is a high-throughput method and requires a short analysis time. The short analysis time increases intersample reproducibility which improves accuracy in cluster analysis. However, chemical isomers cannot be distinguished, and there is a concern about ion suppression due to matrix effects.[13] The use of a multianalytical approach in our study enabled us to exploit the advantages of both techniques and compensate for the limitations that would result from a single technique. Multianalytical approaches are powerful and comprehensive, and they have been used in many studies, for example, investigations of the effect of age on the profile of endogenous metabolites in the urine of male rats[14] and metabolic changes caused by gentamicin-induced nephrotoxicity in rats.[15] Data from ^{1}H NMR and MS were reduced by chemometric methods.

2. Materials and Methods

2.1. Chemicals. Deionized water was obtained from the Millipore Milli-Q purification system (Bedford, MA, USA). The EA.hy926 cell line and C6/36 cells were obtained from the American Type Culture Collection (ATCC) (Manassas, VA, USA). Dulbecco's Modified Eagle's Medium (DMEM) and fetal bovine serum (FBS) were purchased from ATCC (Manassas, VA, USA). Trypsin-EDTA (0.5%, 10×) was purchased from GIBCO (Auckland, NZ). Phosphate Buffer Saline (PBS) (10×) (containing 1.37 M NaCl, 27nM KCl, and 100 mM phosphate buffer) and 0.1 M Na_3PO_4 at pH 7.0 were obtained from first Base (Singapore). D_2O containing 0.05 wt % 3-trimethylsilylpropionic-2,2,3,3-d_4 acid, sodium salt (TSP), crystal violet (CV), L-15, and Roswell Park Memorial Institute (RPMI) media were purchased from Sigma-Aldrich (St. Louis, MO, USA). Chloroform-D with silver foil was purchased from Cambridge Isotope Laboratories, Inc. (Andover, MA, USA). HPLC grade acetonitrile (ACN) and analytical grade ethanol were purchased from Fisher Scientific (Fair Lawn, New Jersey, USA) and analytical grade chloroform and methanol from Tedia (Fairfield, OH, USA). Ammonium acetate was obtained from Merck (Darmstadt, Germany). Carboxy methyl cellulose (CMC) was obtained from Calbiochem (EMDChemicals Inc., USA).

2.2. Cell and Virus Culture.

2.2.1. Cultivation of EA.hy926. EA.hy926 cells were grown according to standard culture practices[16,17] in DMEM with 10% v/v FBS. Cells were maintained in a humidified incubator with 5% CO_2 in a 25 cm^2 tissue culture flask with vented cap at 37 °C. They were subcultured when they reached 80−90% confluence by trypsinization. Briefly, the method involved washing the cell monolayer twice with 1.0 mL of PBS (1×) followed by a rinse with 1.0 mL of trypsin-EDTA (1×), after which the cells were incubated at 37 °C for 1−2 min to allow detachment of cells from the flask. Thereafter, an equal volume of fresh growth medium was added to suspend the detached cells in solution as well as to stop the action of trypsin. The resultant suspension was split into the required portions for subculture.

2.2.2. Dengue Virus Production. C6/36 cells of the *Aedes albopictus* clone (Asian tiger mosquito) were cultivated in a medium containing L-15 with 10% v/v FBS in four culture flasks (75 cm^2) and incubated at 28 °C with atmospheric CO_2 in a nonhumidified incubator. After ∼95−100% confluence of the cell monolayer, the growth medium in each flask was removed. An aliquot of virus stock (expected to contain $\sim 1 \times 10^6$ pfu/mL) (1.0 mL) of each serotype (DEN-1, DEN-2, DEN-3, and DEN-4) was added into each flask and left to incubate at 37 °C for 1 h, with gentle rocking of the flasks every 15 min to increase the rate of viral attachment to the cell membrane. Maintenance medium containing L-15 with 2% v/v FBS was then used to bathe the infected cells.

The infected cells were then incubated at 28 °C with 5% CO_2 in a humidified incubator until cytopathic effects (CPE) were observed in the cells infected by the different viral serotypes. DEN-1-infected C6/36 typically show CPE within 7−9 days postinfection (p.i.); 3−4 days for DEN-2; 9−10 days for DEN-3; and 5 days for DEN-4. After observation of CPE in the infected C6/36 cells, the pH of the maintenance medium was adjusted to 6.8−8.2 by dropwise addition of NaOH (0.5 M) in the presence of phenyl red indicator (until the medium changed from yellow to light red). The maintenance medium was centrifuged for 5 min at 1500 rpm and 4 °C, and the supernatant (containing the virus) was collected and filtered. It was then kept in 1.0 mL aliquots, snap-frozen with −80 °C ethanol, and finally stored at −80 °C.

2.2.3. Dengue Virus Titration. The virus titer of the supernatant corresponding to each viral serotype was determined by a plaque assay using BHK-21, kidney cells of golden Syrian hamster (*Mesocricetus auratus*) (John Aaskov lab, QUT, Australia) cultivated in a medium containing 10% FBS v/v in RPMI in four T-75 culture flasks at 37 °C in a humidified incubator with 5% CO_2. Once confluence was reached, the cells were subcultured in four 24-well plates. An aliquot of virus stock (1.0 mL) (of each serotype) was diluted 10-fold serially six times and gently pipetted into each well according to the illustration shown in Figure 1. Each plate (for each serotype) was incubated at 37 °C in 5% CO_2 in a humidified incubator for an hour, with gentle rocking every 15 min to allow the virus to infect the cells. Excess virus was removed by washing with 1.0 mL of PBS (1×) before 1.0 mL of carboxy-methyl cellulose (CMC) was added to each well. The plates were then incubated at 37 °C in 5% CO_2 in a humidified incubator again. After observation of CPE in the cells, they were stained with crystal violet (CV). On the basis of the staining, the optimum concentration plaques were selected and counted. The total number of plaques for a set of triplicates was counted, averaged, and multiplied by the dilution factor to find the concentration of virus in the harvested supernatant in pfu/mL. The formula is $p \times 10^n \times 10$, where p = average number of plaques counted and n = dilution factor.

2.3. Infection of EA.hy926 Cells with Dengue Virus. EA.hy926 cells were subcultured into four 6-well plates and infected with the dengue virus at multiplicity of infection (MOI) = 1. The cells on each plate were infected with a different virus serotype. Briefly, the cells were washed with PBS (1×) twice before 1.0 mL of stock virus was gently added into each well. The cells were then incubated at 37 °C in 5% CO_2 in a humidified incubator, with gentle rocking every 15 min. Excess virus was removed by washing with 1.0 mL of PBS (1×) before bathing the cells in 5.0 mL of maintenance medium (2% FBS in DMEM). They were then incubated at the same conditions.

2.4. Extraction of Metabolites (Sample Collection). In metabolomics, the aim is to profile or quantify all the small molecular weight metabolites in the sample to understand how metabolites and their interactions influence the phenotype.[18,19] This implies profiling all the intracellular and extracellular metabolites. In this study, extracellular metabolites in the media were studied by assessing the culture media. The main challenge in measurement of intracellular metabolites is the rapid turnover of intracellular metabolites, so it requires a rapid

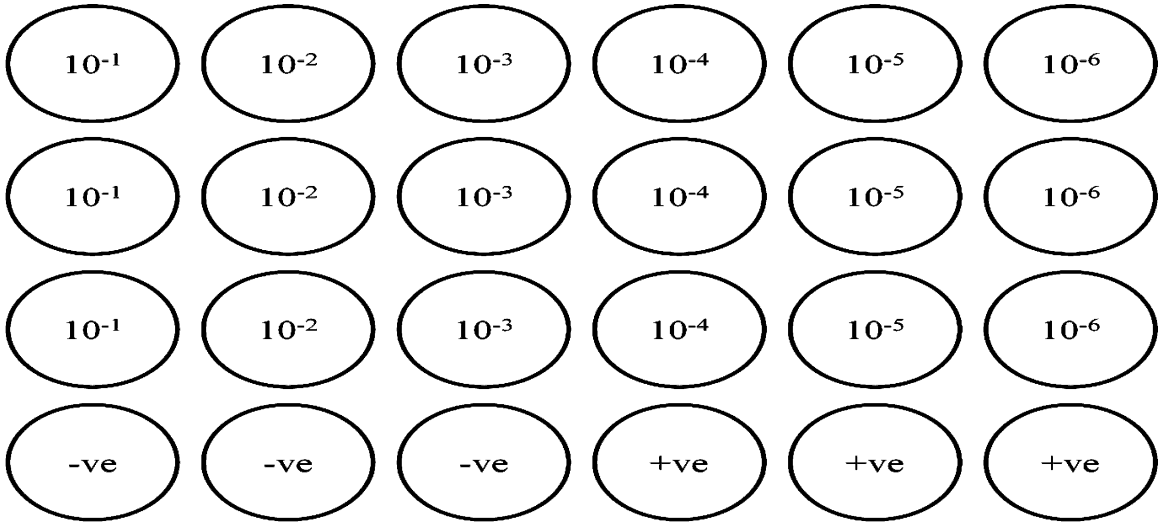

Figure 1. Illustration of the distribution of diluted virus stock for a 24-well plate. An amount of 100 μL of each concentration was pipetted into each well. −ve: negative control (1 × PBS). +ve: positive control (undiluted virus stock).

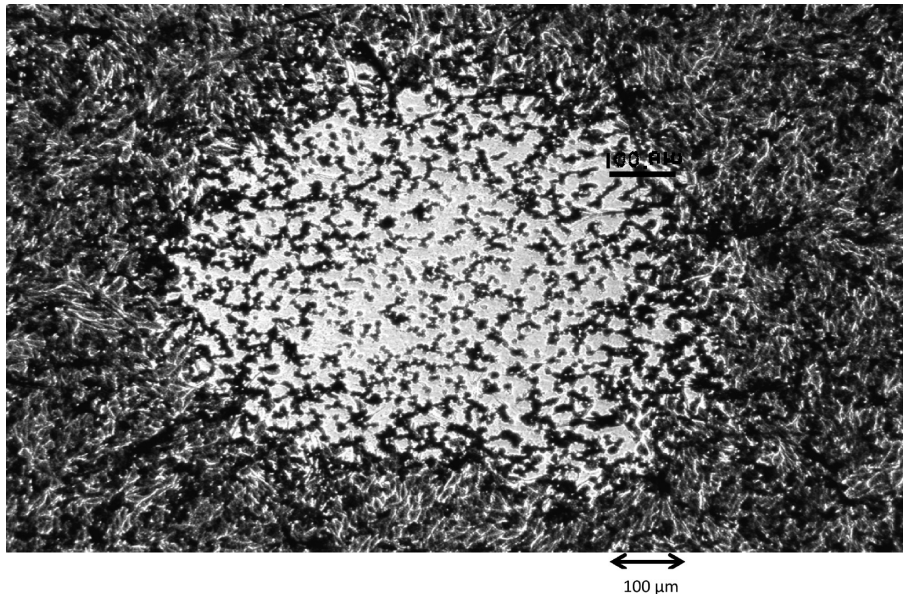

Figure 2. Sample of a single plaque at 20× magnification.

quenching technique and is also time-consuming.[18,20] While intracellular and extracellular metabolites can play different roles,[19] metabolites which are secreted, excreted, or not taken up by the cells clearly reflect the cellular metabolic activity.[18] Analysis of the medium also referred to as footprinting can be used to study the metabolic activity of an organism instead of analyzing the intracellular metabolism because the components in the medium are a reflection of the organism's metabolic activity and the turnover time of metabolites in the medium is not as fast as for intracellular components; therefore, the need for rapid quenching can be avoided.[18,20] On the basis of this literature information, our study focuses on analysis of the media (otherwise known as analysis of the exometabolome) in which the cells grew.

Aliquots (1.0 mL) of the culture medium were drawn from each well at intervals of 6, 24, and 48 h p.i. into individual 15 mL centrifuge tubes. The wells were topped with 1.0 mL of fresh maintenance medium after withdrawal of the test samples. Samples collected were immediately stored at −20 °C. This procedure was repeated another 5 times on 5 other days to test for interday reproducibility. Media were extracted following the method by Miccheli et al.;[10] i.e., to each of the 1.0 mL portions of collected culture medium, 2:1 cold CH_3OH:$CHCl_3$ (3.0 mL) mixture was added followed by $CHCl_3$ (1.0 mL). The resultant mixture was centrifuged at 7000 rpm, 4 °C, for 20 min to allow clear separation between the aqueous and organic layers. The two layers were separated, freeze-dried, and analyzed separately later.

2.5. Sample Preparation for ^{1}H NMR Spectroscopy and HPLC-MS. Aqueous portions were reconstituted with 700 μL of phosphate buffered D_2O (containing 0.05% TSP) at pH 7, and organic portions were reconstituted with 700 μL of $CDCl_3$. The entire sample was sonicated for 5 min at 4 °C to improve dissolution of metabolites and then centrifuged at 7000 rpm for 5 min at 4 °C to remove solid particles.

2.6. Analysis of Samples by ^{1}H NMR Spectroscopy. Reconstituted samples were analyzed using a Bruker 500 MHz Ultrashield spectrometer to obtain one-dimensional ^{1}H NMR spectra at

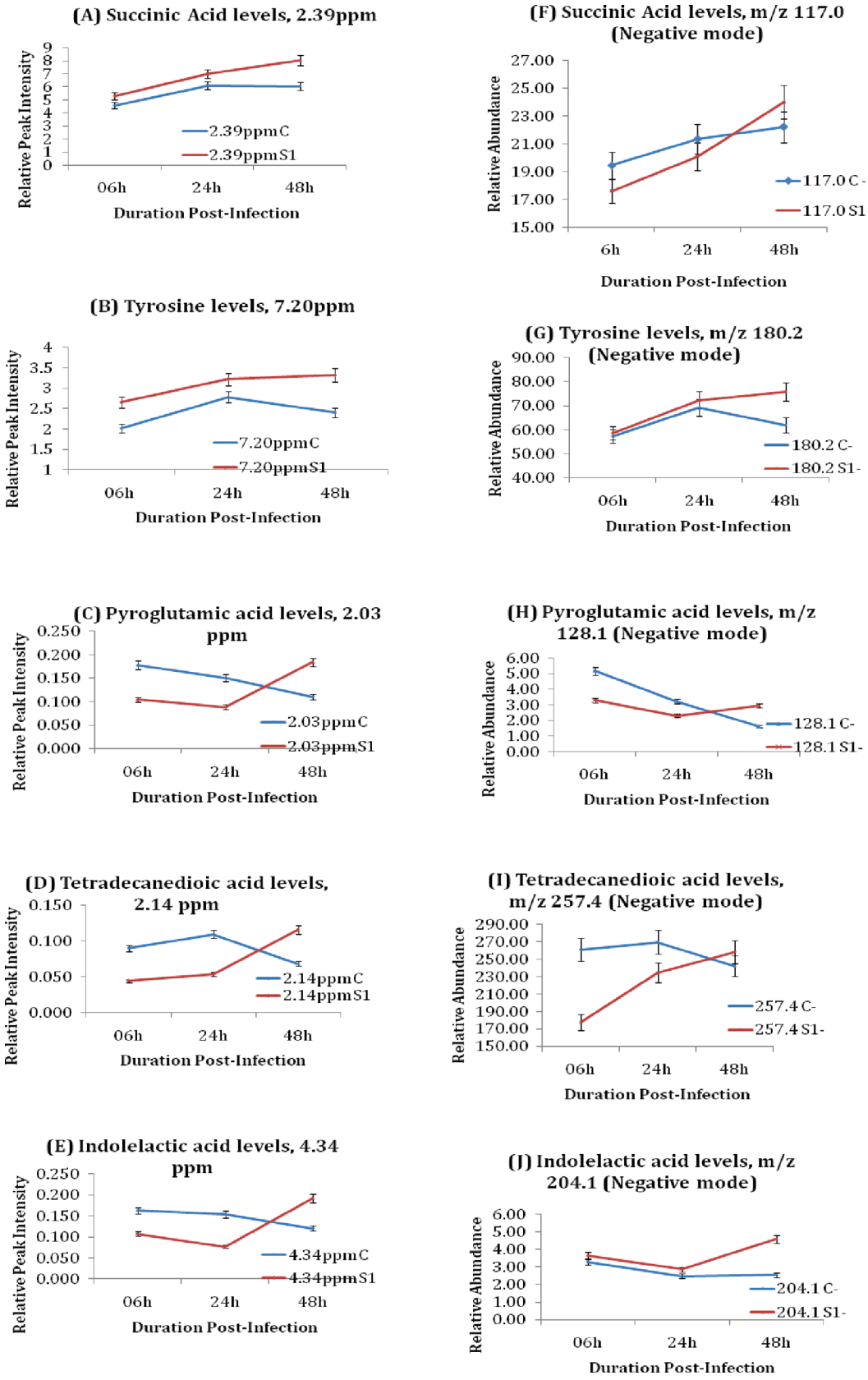

Figure 3. Graphical representation of the variation of metabolites identified in media cells infected with DEN-1 and control cells. Graphs A and F show succinic acid, B and G tyrosine, C and H pyroglutamic acid, D and I tetradecanoic acid; and E and J indolelactic acid. One HMR data is represented by graphs A–E, and MS data are shown in graphs F–J.

an observation frequency of 500 MHz. Aqueous samples were analyzed using a presaturation pulse sequence (relaxation decay −90° acquisition). A secondary radio frequency irradiation of 2 s was applied during the relaxation delay to reduce the peak due

Table 1. Metabolites Identified in Aqueous (*) and Organic (^) Extracts of Growth Medium Bathing Uninfected EA.hy926 (C) and EA.hy926 Infected with Each of 4 DEN Serotypes (S)[a]

identified compound	chemical shift, ppm		relative peak intensity at duration p.i. (h) 06	24	48	*m*/*z*/ionization mode (±)		relative abundance at duration p.i. (h) 06	24	48
			DEN-1-infected EA.hy926							
1* Succinic acid	2.39	C	4.59 ± 1.36	6.10 ± 2.36	6.06 ± 1.11	117.0 (−)	C	19.45 ± 3.73	21.35 ± 3.66	22.22 ± 3.87
		S1	5.30 ± 1.55	7.01 ± 1.18	8.03 ± 2.94		S1	17.59 ± 1.85	20.10 ± 3.71	23.99 ± 5.39
2* Tyrosine	7.20	C	2.02 ± 0.25	2.78 ± 0.74	2.40 ± 0.34	180.2 (−)	C	57.34 ± 6.51	69.23 ± 7.30	61.90 ± 4.50
		S1	2.66 ± 0.42	3.22 ± 0.19	3.32 ± 0.85		S1	58.69 ± 5.27	72.35 ± 4.51	75.71 ± 8.82
3^ Pyroglutamic acid	2.03	C	0.18 ± 0.06	0.15 ± 0.05	0.11 ± 0.05	146.1 (−)	C	1.43 ± 0.62	0.90 ± 0.64	0.46 ± 0.44
		S1	0.10 ± 0.05	0.09 ± 0.04	0.18 ± 0.04		S1	1.23 ± 0.49	0.84 ± 0.26	1.14 ± 0.95
4^ Tetradecanedioic acid	2.14	C	0.09 ± 0.04	0.11 ± 0.05	0.07 ± 0.04	257.4 (−)	C	261.24 ± 14.92	269.44 ± 15.10	242.11 ± 11.60
		S1	0.04 ± 0.03	0.05 ± 0.03	0.12 ± 0.03		S1	177.62 ± 10.94	234.55 ± 10.08	258.23 ± 13.67
5^ Indolelactic acid	4.34	C	0.16 ± 0.09	0.15 ± 0.07	0.12 ± 0.06	204.1 (−)	C	3.30 ± 1.42	2.49 ± 1.68	2.55 ± 0.87
		S1	0.11 ± 0.05	0.08 ± 0.04	0.19 ± 0.07		S1	3.66 ± 1.59	2.86 ± 1.51	4.58 ± 1.91
			DEN-2-infected EA.hy926							
1* 3-Methyl-2-oxovaleric acid	1.11	C	0.63 ± 0.15	0.99 ± 0.28	0.84 ± 0.38	129.1 (−)	C	50.40 ± 8.85	85.64 ± 7.44	51.13 ± 4.12
		S2	0.76 ± 0.10	0.93 ± 0.37	0.94 ± 0.26		S2	60.30 ± 6.10	65.91 ± 4.99	59.75 ± 2.49
2^ Alanine	1.48	C	0.71 ± 0.24	0.56 ± 0.10	0.47 ± 0.14	90.0 (+)	C	1.08 ± 0.48	0.78 ± 0.39	0.59 ± 0.37
		S2	0.69 ± 0.30	0.51 ± 0.20	0.67 ± 0.17		S2	0.98 ± 0.29	0.62 ± 0.33	0.74 ± 0.39
			DEN-3-infected EA.hy926							
1* Isoleucine	0.93	C	4.58 ± 1.72	5.53 ± 1.29	5.94 ± 0.80	132.1 (+)	C	150.13 ± 5.79	156.78 ± 3.80	166.84 ± 3.58
		S3	4.96 ± 1.30	5.85 ± 1.10	7.91 ± 0.78		S3	164.64 ± 5.40	196.41 ± 5.66	227.07 ± 9.55
2* Acetoacetic acid	2.28	C	1.76 ± 0.55	2.35 ± 0.90	2.03 ± 0.75	101.0 (−)	C	8.22 ± 1.81	10.43 ± 3.25	8.10 ± 1.03
		S3	1.94 ± 0.57	2.07 ± 0.88	3.22 ± 0.70		S3	8.08 ± 0.96	10.11 ± 1.64	11.93 ± 1.76
3* Serine	3.92	C	42.43 ± 18.25	43.40 ± 11.36	35.94 ± 8.20	104.0 (−)	C	66.59 ± 4.96	68.20 ± 6.50	55.92 ± 3.09
		S3	41.14 ± 8.66	40.82 ± 10.05	57.17 ± 4.45		S3	67.18 ± 3.26	71.93 ± 4.02	75.79 ± 2.56
4* Tryptophan	7.27	C	0.47 ± 0.20	0.59 ± 0.15	0.52 ± 0.20	203.1 (−)	C	73.02 ± 10.31	80.80 ± 7.35	73.39 ± 6.00
		S3	0.63 ± 0.09	0.60 ± 0.33	0.97 ± 0.22		S3	84.11 ± 6.52	81.16 ± 10.23	85.97 ± 3.76
5* Phenylalanine	7.38	C	1.49 ± 0.33	1.51 ± 0.28	1.37 ± 0.31	166.1 (+)	C	87.62 ± 2.88	95.64 ± 2.77	94.77 ± 6.62
		S3	1.51 ± 0.18	1.54 ± 0.44	2.18 ± 0.26		S3	100.41 ± 2.81	108.22 ± 8.23	133.44 ± 6.96
6* Hippuric acid	7.56	C	0.65 ± 0.27	0.67 ± 0.14	0.53 ± 0.26	178.0 (−)	C	5.88 ± 1.11	5.66 ± 1.53	5.38 ± 0.83
		S3	0.72 ± 0.12	0.68 ± 0.33	1.03 ± 0.19		S3	5.92 ± 1.36	6.06 ± 0.97	6.84 ± 1.39
7^ Cholesterol	0.95	C	0.68 ± 0.43	0.48 ± 0.11	0.40 ± 0.11	385.0 (−)	C	158.36 ± 8.22	145.98 ± 8.46	141.14 ± 8.23
		S3	0.55 ± 0.14	0.37 ± 0.13	0.53 ± 0.12		S3	152.27 ± 9.29	146.89 ± 10.50	166.09 ± 9.52
8^ Hexadecanedioic acid	1.79	C	0.28 ± 0.14	0.26 ± 0.09	0.18 ± 0.05	285.4 (−)	C	192.58 ± 10.55	160.09 ± 7.31	155.71 ± 9.22
		S3	0.24 ± 0.12	0.15 ± 0.04	0.26 ± 0.09		S3	161.70 ± 7.82	138.22 ± 6.89	202.64 ± 9.40
			DEN-4-infected EA.hy926							
1* Isoleucine	1.28	C	1.46 ± 0.45	1.68 ± 0.38	1.26 ± 0.68	132.10 (+)	C	204.13 ± 5.79	220.78 ± 13.80	166.84 ± 13.58
		S4	1.29 ± 0.36	1.85 ± 0.36	1.89 ± 0.59		S4	160.04 ± 5.91	256.38 ± 7.53	277.04 ± 5.13
2^ Nonadecanoic acid	1.30	C	4.73 ± 1.49	4.46 ± 1.46	0.61 ± 0.17	297.5 (−)	C	72.04 ± 0.94	59.93 ± 1.94	52.18 ± 6.71
		S4	7.47 ± 3.28	3.33 ± 1.39	0.70 ± 0.33		S4	100.32 ± 3.59	55.18 ± 4.81	58.02 ± 8.19
3^ Pentacosanoic acid	2.35	C	0.99 ± 0.33	1.08 ± 0.80	0.64 ± 0.32	381.7 (−)	C	13.04 ± 7.61	16.32 ± 7.57	10.76 ± 4.99
		S4	1.80 ± 0.89	0.72 ± 0.22	0.85 ± 0.58		S4	20.44 ± 10.34	11.48 ± 6.60	12.33 ± 5.13
4^ Kynurenine	7.39	C	0.38 ± 0.19	0.35 ± 0.17	0.27 ± 0.13	207.2 (−)	C	42.89 ± 3.13	32.47 ± 1.09	33.11 ± 0.64
		S4	0.66 ± 0.46	0.23 ± 0.12	0.34 ± 0.21		S4	36.78 ± 4.42	36.09 ± 1.67	37.96 ± 0.85

[a] Values are given as mean ± SD; the significant difference between uninfected and infected EA.hy926 is based on two-tailed student's *t*-test where $p < 0.05$.

to water resonance, and 64 scans were collected. Organic samples were analyzed similarly but without solvent suppression. The ^{1}H spectra obtained from all samples were manually processed for auto-phase correction using TOPSPIN software (Bruker Biospin).

2.7. Analysis of Samples by Direct Injection MS (DIMS). DIMS analysis of all samples was performed on an Agilent 1200 series system including a degasser, binary pump, temperature-controlled autosampler, and temperature-controlled column compartment. It was coupled to an Agilent 6410 Triple Quad mass spectrometer system with an electrospray ionization (ESI) source. The mobile phase used consisted of A (90% ACN, 0.1% acetic acid, 0.1% ammonium acetate, 9.8% deionized water) and B (deionized water with 0.1% acetic acid and 0.1% ammonium acetate). Isocratic elution was used at 50% A and 50% B, and the total run time was 3 min. The samples were analyzed in full scan mode ($m/z = 70-1000$) in both positive and negative modes during LC−MS analysis.

2.8. Chemometric Analysis. All ^{1}H NMR spectra obtained were manually phased and baseline-corrected using MestReNova software (Mestrelab Research, Santiago de Compostela, Spain). Aqueous sample spectra were normalized to the TSP peak at $\delta = 0.00$, and organic sample spectra were normalized to the $CHCl_3$ peak at $\delta = 7.26$. Peaks between $\delta = 0$ and $\delta = 9.00$ were picked for the spectra of the aqueous samples, while those between $\delta = 0.00$ and $\delta = 11.10$ were picked for the spectra of the organic samples. The chemical shifts of the picked peaks and corresponding peak intensities were tabulated, aligned, and consolidated in Microsoft Excel (Microsoft Corporation, Redmond, WA) and analyzed by principal component analysis (PCA) using SIMCA-P+ (Umetrics, Umea, Sweden). The resultant loading plots were studied to identify the chemical shifts responsible for the separation in the score plots.

For DIMS, the total ion chromatograms (TICs) captured in Agilent Mass Hunter Qualitative Analysis were exported to Microsoft Excel with mass-to-charge ratios from 70 to 1000 versus the relative abundances. They were consolidated and analyzed by PCA using SIMCA-P+ (Umetrics, Umea, Sweden). The resultant loading plots were used to identify the m/z values that gave rise to separation in the score plots.

2.9. Statistical Analysis and Peak Assignment. Two-tailed student t tests were conducted on both ^{1}H NMR and LC−MS data to compare control (uninfected) cells and infected cells (from a particular DEN serotype). Chemical shifts or m/z values of $p \leq 0.05$ were considered to be of statistical significance. Compound identification based on chemical shifts and m/z values was by consultation of online databases. The Human Metabolome Database (HMDB)[21,22] and BioMagResBank (BMRB)[23] were used for NMR data, and the METLIN Metabolite Database[24] was used for MS m/z values. Furthermore, previous works associated with peak assignment by Nicholson et al.[25] and Teng et al.[26] were also referred to.

3. Results

3.1. Plaque Assay. The plaque assay revealed the virus titers of each serotype to be ~1.0×10^6 pfu/mL. Hence, EA.hy926 cells were seeded at 5.0×10^5 cells/mL one day prior to infection. Upon doubling, there was a 1:1 virion/cell ratio, and MOI = 1 was achieved. A single plaque at 20× magnification is shown in Figure 2.

3.2. Results Obtained from Media Extracts. Results obtained from this study indicated fingerprints that can be attributed to a specific dengue virus serotype because patterns (PCA plots) obtained from samples infected with the different dengue virus serotypes clearly separated from each other and also separated from controls as shown in Figures 8 and 9. Several metabolites (mainly amino acids, dicarboxylic acids, and fatty acid) were also found to vary as explained below.

3.2.1. ^{1}H NMR Spectroscopy and MS Results of Aqueous and Organic Extracts. ^{1}H NMR and mass spectra of aqueous and organic sample extracts showed differences from those of the aqueous and organic control extracts, and the metabolites that were significantly different in uninfected and infected EA.hy926 were identified. From the results obtained, it was evident that infection with dengue virus generally affects amino acid metabolism, fatty acid metabolism, and the tricarboxylic acid cycle. The details are explained below.

In samples infected with DEN-1 virus, tyrosine, succinic acid, pyroglutamic acid, indolelactic acid, and tetradecanoic acid were found to have increased compared to control samples. This is illustrated in Figure 3 and Table 1. For samples infected with DEN-2 virus, alanine increased compared to controls, while 3-methyl-2-oxovaleric acid increased slightly in controls but returned to about the starting value. In samples infected with DEN-2, the increase in 3-methyl-2-oxovaleric acid was less than in control cells as shown in Figure 4 and Table 1.

For EA.hy926 infected with DEN-3, the amino acids isoleucine, serine, tryptophan, and phenylalanine were found at increased levels compared to those in uninfected EA.hy926 (control). Acetoacetate, hippuric acid, hexadecanedioic acid, and cholesterol were also found at elevated levels in the media of infected cells compared to that of the controls. This is illustrated in Figures 5 and 6 and Table 1. Media from samples infected with DEN-4 showed elevated levels of isoleucine, kynurenine, nonadecanoic acid, and pentacosanoic acid compared to controls. This is as shown in Figure 7 and Table 1.

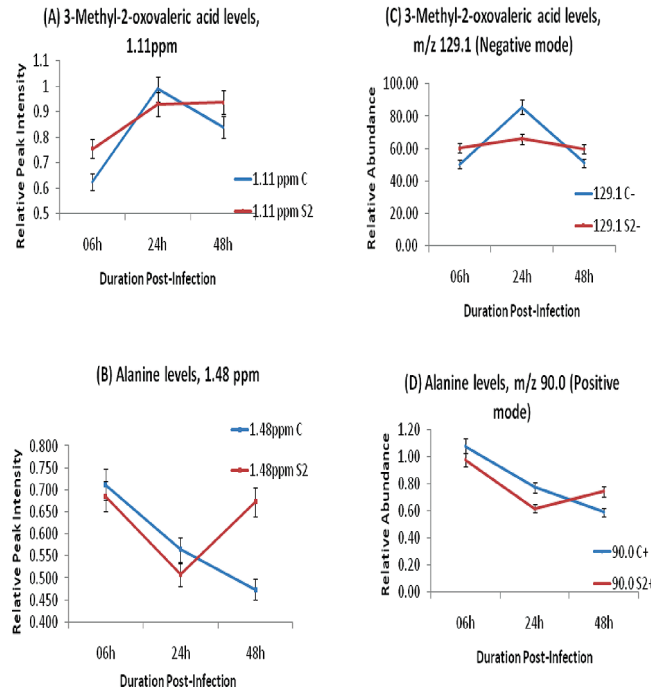

Figure 4. Graphical representations of the variation of some metabolites identified in the growth medium of uninfected EA.hy926 (blue) and DEN-2-infected EA.hy926 (red). (A, C): 3-Methyl-2-oxovaleric acid. (B, D): Alanine. Graphs are based on ^{1}H NMR (A, B) and MS (C, D) data.

Useful information on the m/z values of the aqueous components was obtained from the extracted mass spectra of the aqueous samples' total ion chromatograms (TICs) in DIMS. In ^{1}H NMR, several peaks were observed, and in DIMS a large number of m/z values were obtained. The results were therefore analyzed using principal component analysis (PCA).

3.2.2. Principal Component Analysis (PCA). Figure 8 shows the three-dimensional (3D) PCA scatter plots obtained from ^{1}H NMR data of the aqueous and organic samples collected at 48 h p.i. Figure 9 show scatter plots for an individual virus serotype and a control sample obtained using MS data. Scatter plots comparing control cells and all samples infected with each serotype (Figure 8) and scatter plots comparing controls and cells infected with one particular serotype were generated (Figure 9). All the five data sets (controls with the four sets of cells each infected with one of the four DEN serotypes) clearly separated. The same pattern was observed for plots corresponding to aqueous and organic samples extracted at 6 and 24 h p.i. in both NMR and MS data. When individual serotype data were compared with control samples, there was a clear separation between the samples infected with a particular viral serotype (e.g., DEN-1) and control. Two distinct clusters were observed for both aqueous and organic data and in all four serotypes as well as for both ^{1}H NMR or MS derived data.

Interday repeatability was achieved for both aqueous and organic extracts at 24 and 48 h p.i. for both ^{1}H NMR data and MS data. There was a clear distinction among the data groups, and the same observation was achieved for MS data in negative mode.

Peaks of interest were generated using SIMCA-P+ and tested for statistical significance using the student t test. The final consolidated list of peaks, chemical shifts, and m/z values (found in aqueous and organic extracts) is tabulated in Table 1.

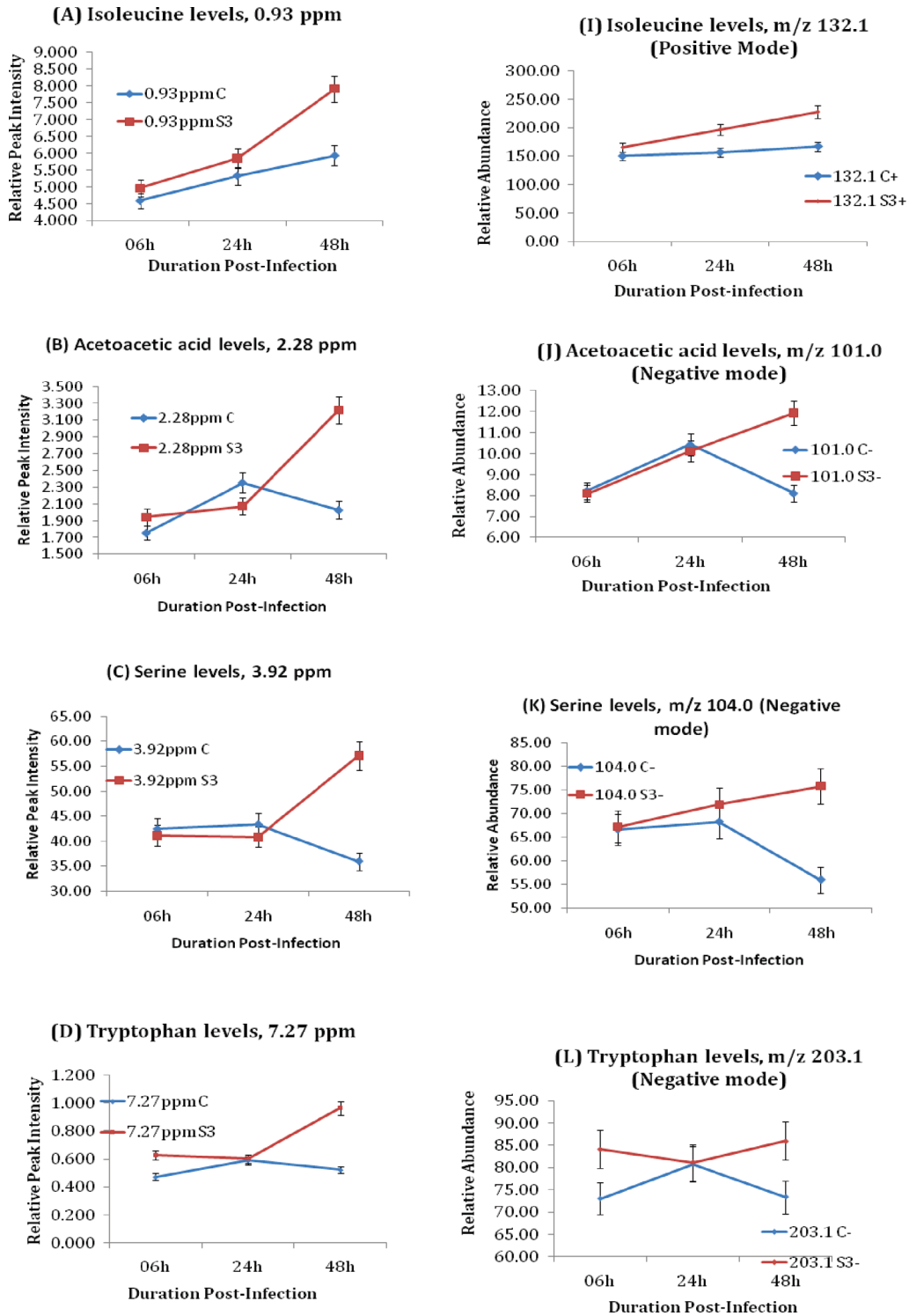

Figure 5. Graphical representations of metabolites identified in the growth medium of uninfected EA.hy926 (blue) and DEN-3-infected EA.hy926 (red). (A, I) Isoleucine, (B, J) acetoacetic acid, (C, K) serine, and (D, L) tryptophan. (Graphs are based on ^{1}H NMR (A−D) and MS (I−L) data.)

4. Discussion

In this study, ^{1}H NMR and MS analyses were employed to study the metabolic profiles of EA.hy926 infected with different dengue serotypes. The results obtained revealed finger/footprints that can be attributed to specific dengue serotypes and variations in the amounts of certain metabolites (like amino acids, fatty acids, keto acids, indole acids, acyl glycines, and cholesterol) in the media from infected cells compared to control cells. Some of the metabolites identified are as shown in Figures 3−7 and in Table 1. From the footprinting patterns/results, it was evident that different metabolic pathways are affected when the cells are infected with a particular serotype, thus there may be distinct effects of infection by specific dengue virus serotypes. Our observations are in agreement with

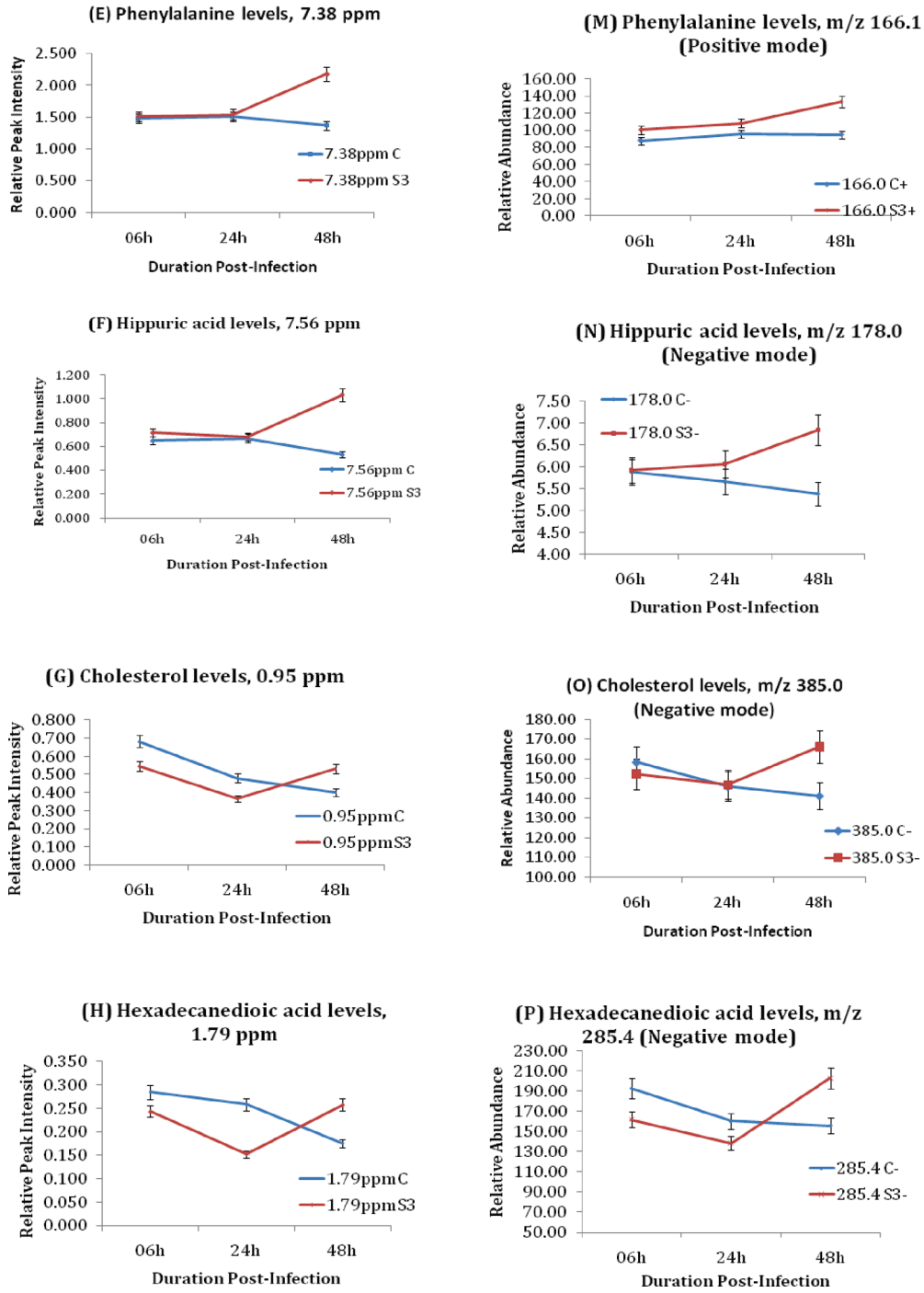

Figure 6. Graphical representations of metabolites identified in the growth medium of uninfected EA.hy926 (blue) and DEN-3-infected EA.hy926 (red). (E, M) Phenylalanine, (F, N) hippuric acid, (G, O) cholesterol, and (H, P) hexadecanedioic acid. Graphs are based on ^{1}H NMR (E−H) and MS (M−P) data.

previous results obtained by gas−liquid chromatography on monkey kidney cells infected with the same four serotypes of dengue viruses described by Brooks et al.[27] Different serotypes may have different severity of infection thus leading to these differences observed. The observed differences may also be the reason that different viral diseases could alter the host cell metabolism or body response in different ways.[27] In the future, more metabolites will be identified to determine if there are different metabolites or if the amounts produced are different for each serotype.

Generally, metabolite levels are regulated by homeostasis; however, dengue infection has been reported in the literature to cause abnormalities in homeostasis,[28] and therefore the imbalance in metabolite amounts as observed in our study is in agreement with literature reports.

The amount of metabolites in the media is dependent on their uptake or inability to be taken up as well as the secretion and excretion of metabolites from the cells. Furthermore, vascular leakage, the increased permeability of the cell membrane associated with dengue infection, may cause cell contents to leak into the medium. Profiling the media components therefore can give an insight into the metabolic process of the cells because it is a good reflection of the metabolic status of the cells.

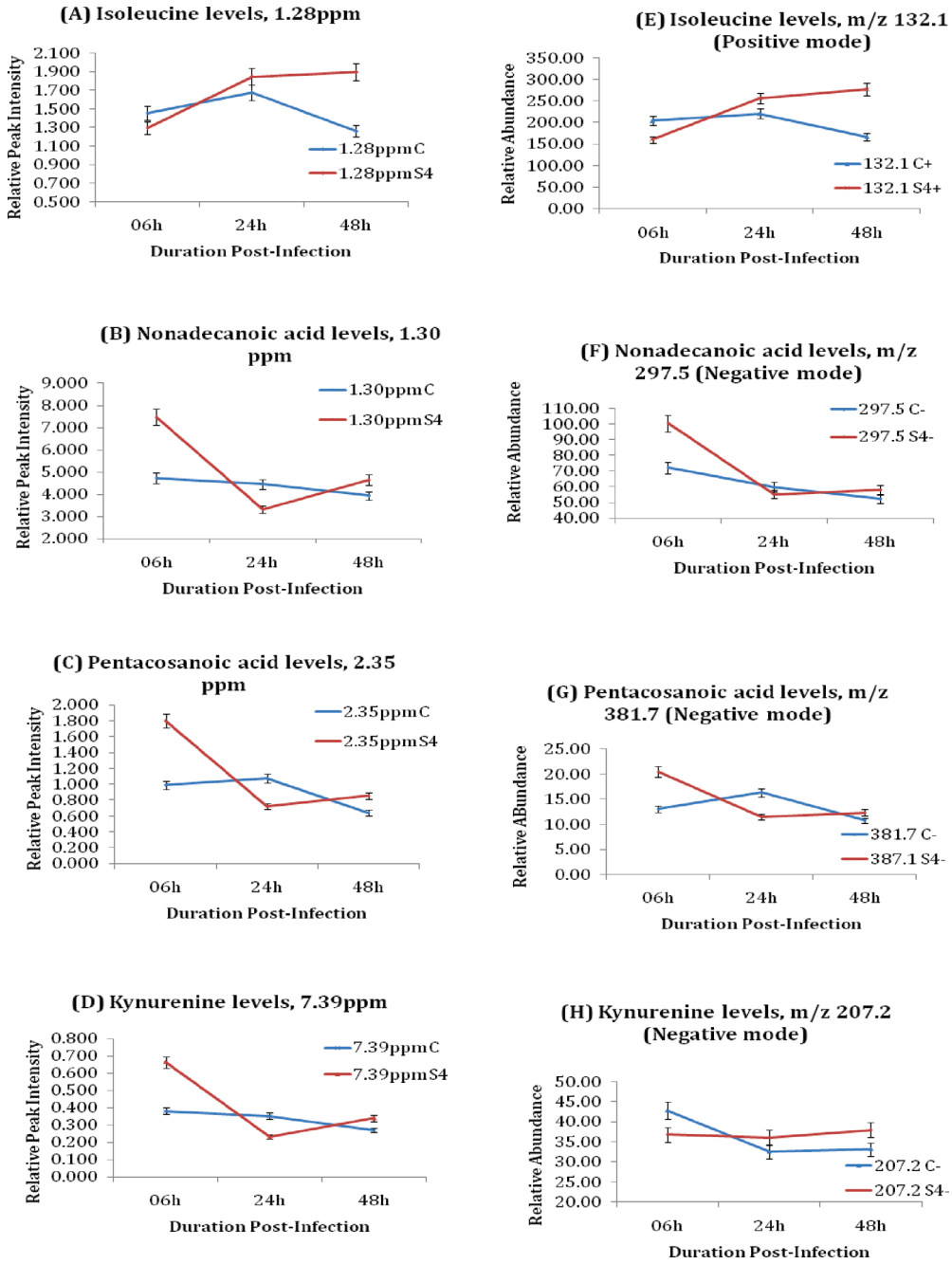

Figure 7. Graphical representations of metabolites identified in the growth medium of uninfected EA.hy926 (blue) and DEN-4-infected EA.hy926 (red). (A, E) Isoleucine, (B, F) nonadecanoic acid, (C, G) pentacosanoic acid, and (D, H) kynurenine. Graphs are based on ^{1}H NMR (A−D) and MS (E−H) data.

Variations in the metabolites amounts in infected cells compared to control cells represent the biochemical reactions in the cell and therefore can give a clear picture of what is happening in the cells. From these variations, the pathways affected can be deduced, and the mode of action of the virus can be better understood. In this study, the metabolites' levels (in terms of relative peak intensity (for ^{1}H NMR) and relative abundance (for MS)) were monitored up to 48 h p.i. to determine if there were changes in infected cells compared to uninfected cells. Changes in metabolite amounts were observed mainly in amino acids, dicarboxylic acids, and fatty acids as explained below.

4.1. Amino Acids. An increased level of the aromatic amino acid tyrosine was observed in media of samples infected with DEN-1 compared to controls, implying a disruption of its metabolism. Conversion of phenylalanine to tyrosine is an important step in the catabolism of phenylalanine as well as in the synthesis of tyrosine (refer to phenylalanine metabolic pathway, e.g., http://www.genome.jp/dbget-bin/www_bget?map00360). The elevated levels of tyrosine are in agreement with the high levels of phenylalanine from which it is produced. Such high amounts would have an effect on the amount of acetoacetate produced, and in fact increased levels of acetoacetate were observed in media of samples infected with DEN-3 where the amino acid phenylalanine was also at elevated levels.

Elevated levels of alanine were observed in the medium of DEN-2-infected EA.hy926. In normal alanine metabolism,

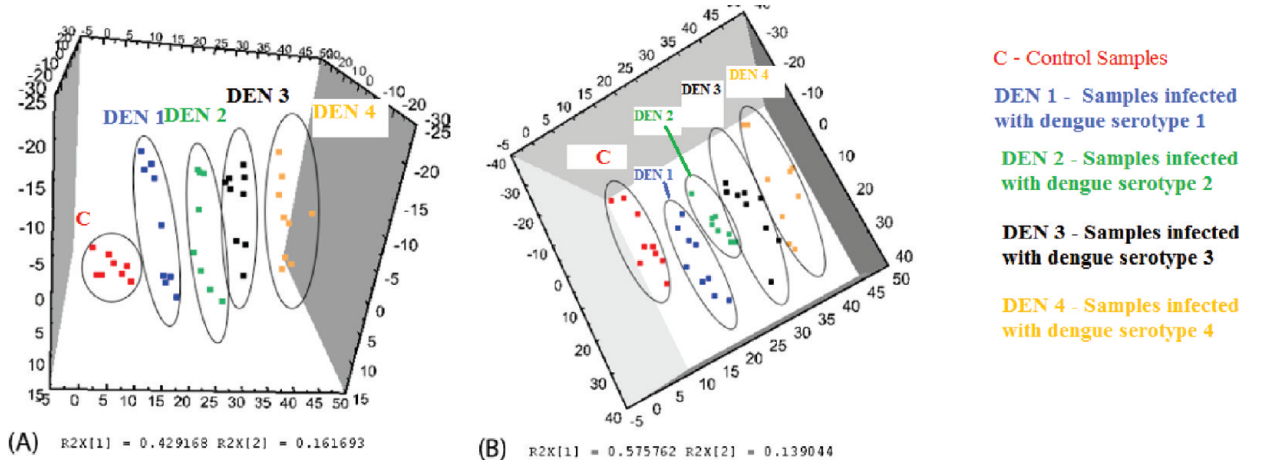

Figure 8. 3D score plots type (1) of aqueous (A) and organic (B) portions of growth medium extracted from cultures of uninfected EA.hy926 and those infected with the four serotypes of dengue virus, based on ^{1}H NMR data, at 48 h p.i. Red, uninfected EA.hy926; blue, EA.hy926 infected with DEN-1; green, DEN-2; black, DEN-3; and yellow, DEN-4 ($n = 9$ each).

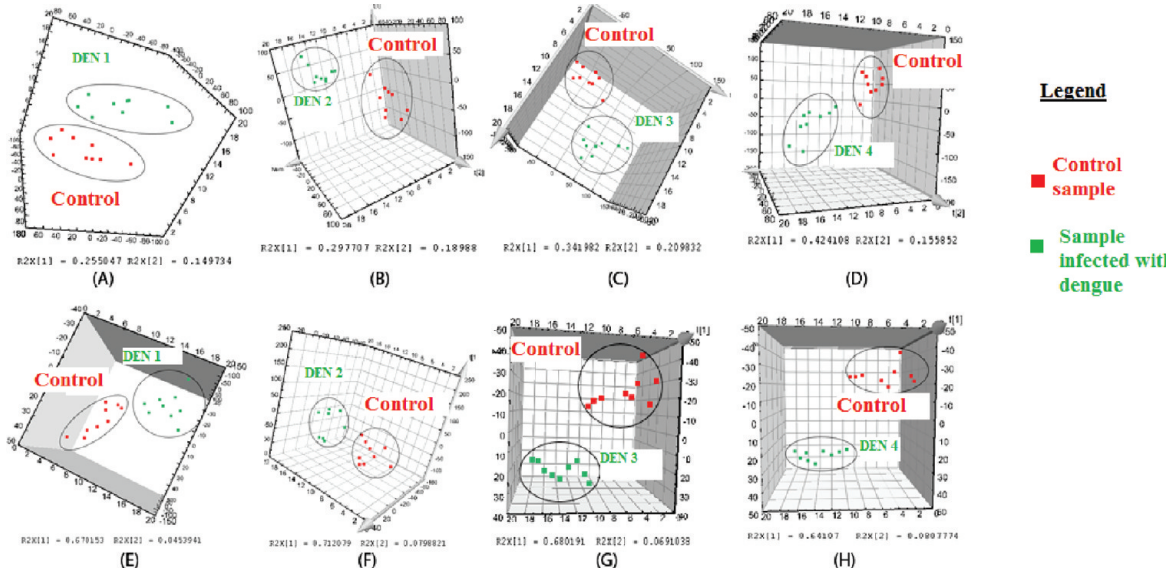

Figure 9. 3D score plot type (2) of aqueous (A−D) and organic (E−H) portions of growth medium extracted from cultures of uninfected EA.hy926 ($n = 9$) and those infected with DEN-1 (A, E), DEN-2 (B, F), DEN-3 (C, G), and DEN-4 (D, H), $n = 9$ each, at 48 h p.i., based on MS data in positive mode. Red, uninfected EA.hy926; green, infected EA.hy926.

alanine is converted to pyruvate via transamination, which enters the tricarboxylic acid (TCA) cycle for adenosine triphosphate (ATP) production. Hence accumulation of alanine in infected EA.hy926 could be due to interference in alanine catabolism and would be responsible for the observed increase in alanine levels in infected samples compared to controls. This in effect can disrupt the TCA cycle.

For EA.hy926 infected with DEN-3, the essential amino acids isoleucine, tryptophan, and phenylalanine were found at increased levels compared to control cells. Elevated levels of isoleucine were also found in media of samples infected with DEN-4. These increased levels could indicate interference in their catabolism after dengue infection of EA.hy926, so they may not be converted into suitable biomolecules (such as pyruvate, acetyl-coA, and succinyl-coA), which enter the TCA cycle for ATP production. Isoleucine is synthesized from aspartate derived from oxaloacetate (from the TCA cycle). The increased level was probably due to disruption in its catabolism for production of acetylCoA which joins the TCA cycle. Tryptophan is catabolized mainly through the kynurenine pathway.[29] In this pathway, oxidation followed by hydrolysis of tryptophan occurs in series producing kynurenine (refer to the tryptophan pathway, e.g., http://www.genome.jp/dbget-bin/www_bget?map00380) which undergoes further oxidation and hydrolysis releasing alanine in the process. In our study, tryptophan, kynurenine, and alanine increased in samples infected with dengue signifying interference in the kynurenine pathway of tryptophan catabolism. Kynurenine, an intermediate in the conversion of tryptophan, was also found to increase in media of samples infected with DEN-4 compared to controls.

Serine, a nonessential amino acid, increased in samples infected with DEN-3 compared to control samples. It is synthesized from 3-phosphoglycerate and is a precursor of several biomolecules (e.g., it is catabolized to produce glycine and cysteine). Serine also participates in purine and pyrimidine metabolism. Its accumulation signifies interference in its catabolism.

In general, infection with dengue affected the metabolism of the aromatic amino acids phenylalanine, tyrosine, and

tryptophan. Elevated levels of intermediates in these pathways were also noted.

4.2. Tricarboxylic Acid Cycle and Fatty Acid Metabolism. Succinic acid, pyroglutamic acid, tetradecanoic acid, and indolelactic acid increased in DEN-1-infected EA.hy926 compared to control (uninfected) EA.hy926. Indolelactic acid is linked to tryptophan metabolism, which is important because it culminates in eventual production of pyruvate. Pyruvate can then be converted to acetyl-coA, which enters the TCA cycle for energy production. Therefore, increased indolelactic acid levels could lead to decreased production of pyruvate, correspondingly disrupting the TCA cycle and ATP production. Pyroglutamic acid is formed from amino acids, catalyzed by γ-glutamylcyclotransferase,[21] and it is present in minute quantities due to its rare occurrences in human proteins.[30] It is formed from glutamine, glutamate, and γ-glutamylated peptides. Therefore increased production of pyroglutamic acid is associated with problems in glutamine or glutathione metabolism.[31]

Hippuric acid is an acyl glycine formed from acyl CoA, and glycine was found at elevated levels in samples infected with DEN-3. This is in agreement with the observed increase in serine which can be converted into glycine.

Tetradecanedioic acid is a dicarboxylic acid produced in small amounts under normal circumstances due to ω-oxidation of medium chain fatty acids. It can be attached to CoA, and the molecule will undergo β-oxidation finally producing succinic acid which enters the TCA cycle. Increased succinnic acid observed could therefore be a result of ω-oxidation of medium chain fatty acids as a result of DEN-1 infection. 3-Methyl-2-oxovaleric acid was found at elevated levels in DEN-2-infected EA.hy926 cells compared to control cells. It is a product of isoleucine in the valine, leucine, and isoleucine degradation pathway.[32] The increased amount of 3-methyl-2-oxovaleric acid is in agreement with the increased amount of isoleucine also observed in media from samples infected with DEN-3 and DEN-4 since it is a metabolite of isoleucine.

DEN-3-infected cells exhibited an elevated level of hexanedecanedioic acid compared to control samples. It is a dicarboxylic acid whose increased production is linked to increased ω-oxidation as a response to infection. Nonadecanoic acid and pentacosanoic acid levels were present in increased levels in DEN-4-infected EA.hy926, which indicates an interruption in metabolism of these saturated long-chain fatty acids via β-oxidation. Elevated cholesterol levels were also observed. High cholesterol is known to be linked to defects in low-density lipoprotein (LDL) metabolism,[30] which is caused by the absence or dysfunction of LDL receptors. This can happen when receptor synthesis does not occur at all or when newly synthesized protein does not successfully reach the plasma membrane due to faulty transport from the Golgi apparatus or faulty Golgi processing. At this stage, the increase in cholesterol levels which is a metabolic manifestation was observed.

In general, infection with dengue virus affected the isoleucine degradation pathway, tricarboxylic acid cycle, and fatty acid metabolism.

4.3. Overall Evaluation. In all four serotypes, their infection of EA.hy926 resulted in changes in levels of some amino acids; therefore, dengue virus infection affects amino acid metabolism. These changes are probably due to the fact that enzymes involved in amino acid metabolism are affected. This observation is in agreement with results obtained by Kanlaya et al.[5] In their study, glutamate dehydrogenase was found to be downregulated in EA.hy926 infected with DEN-2.[5] Glutamate dehydrogenase is the enzyme responsible for the formation of glutamate from α-ketoglutarate and ammonium ions. Glutamate is the predominant amino acid that donates its amino group to an α-keto acid to synthesize other amino acids in transamination. Therefore, when levels of glutamate dehydrogenase are affected, many amino acids are affected.

For dicarboxylic acids like tetradecanedioic acid and hexadecanedioic acid that showed increased levels in infected cells, they are most likely linked to increased ω-oxidation of fatty acids rather than the normal β-oxidation route. Increased levels of fatty acids like nonadecanoic acid and pentacosanoic acid also point to decreased β-oxidation of fatty acids. Furthermore, hippuric acid could be linked to decreased fatty acid metabolism which involves acyl CoA forming acetyl CoA for ATP production. From our study, it appears that dengue infection is associated with increased ω-oxidation of fatty acids.

5. Conclusion

Studying the exometabolome of EA.hy926 provides new insights into the effects of dengue virus infection since the biochemical profile is a good reflection of the metabolic status of the cells. Our results have demonstrated the feasibility of observing distinct effects of infection even among different viral serotypes, with the help of a multianalytical platform comprised of ^{1}H NMR spectroscopy, MS, and pattern recognition tools like PCA.

There were significant differences in the metabolic profiles of uninfected EA.hy926 compared to those infected with any one of the DEN-1, 2, 3, or 4 serotypes. The biomolecules observed to be different include amino acids, fatty acids, various organic acids, cholesterol, and kynurenine, which are indicative of the possible metabolic pathways affected.

From our study, dengue infection appears to affect amino acid metabolism and the TCA cycle. Furthermore dengue infection was linked to ω-oxidation of fatty acids. In the future, more work will be done to confirm the specific metabolites responsible for the observed patterns in PCA plots, and the pathways affected will be investigated in more detail. Observation of metabolite levels over a longer postinfection duration can be done to further ascertain the trends observed in this study, and the effect of dengue infection on other cell types can be investigated.

Acknowledgment. We acknowledge financial support from the National University of Singapore, Ministry of Education (R-143-000-293-112, R-143-000-382-112, and R-143-000-416-232), A-STAR (SERC PSF 052 101 0044), Singapore Bioimaging Consortium (SBIC 009/2005), National Research Foundation and Economic Development Board (SPORE), Ministry of Defense (R-143-000-416-646), and Environment and Water Industry Development Council (0601-IRIS- 093-08). We would also like to thank the Medicinal Chemistry Program of NUS for equipment support and Agilent Technologies for the generous loan of the LC-MS QQQ system. The authors declare no conflict of interest.

References

(1) Rothman, A. L.; Ennis, F. A. Immunopathogenesis of dengue hemorrhagic fever. *Virology* **1999**, *257* (1), 1–6.

(2) Recker, M.; Blyuss, K. B.; Simmons, C. P.; Hien, T. T.; Wills, B.; Farrar, J.; Gupta, S. Immunological serotype interactions and their effect on the epidemiological pattern of dengue. *Proc. R. Soc. B, Biol. Sci.* **2009**, *276* (1667), 2541–2548.
(3) Liew, K. J. L.; Chow, V. T. K. Microarray and real-time RT-PCR analyses of a novel set of differentially expressed human genes in ECV304 endothelial-like cells infected with dengue virus type 2. *J. Virol. Methods* **2006**, *131* (1), 47–57.
(4) Liew, K. J. L.; Chow, V. T. K. Differential display RT-PCR analysis of ECV304 endothelial-like cells infected with dengue virus type 2 reveals messenger RNA expression profiles of multiple human genes involved in known and novel roles. *J. Med. Virol.* **2004**, *72* (4), 597–609.
(5) Kanlaya, R.; Pattanakitsakul, S. N.; Sinchaikul, S.; Chen, S. T.; Thongboonkerd, V. Alterations in Actin Cytoskeletal Assembly and Junctional Protein Complexes in Human Endothelial Cells Induced by Dengue Virus Infection and Mimicry of Leukocyte Transendothelial Migration. *J. Proteome Res.* **2009**, *8* (5), 2551–2562.
(6) Huang, Y. H.; Lei, H. Y.; Liu, H. S.; Lin, Y. S.; Liu, C. C.; Yeh, T. M. Dengue virus infects human endothelial cells and induces IL-6 and IL-8 production. *Am. J. Trop. Med. Hyg.* **2000**, *63* (1−2), 71–75.
(7) Lei, H. Y.; Yeh, T. M.; Liu, H. S.; Lin, Y. S.; Chen, S. H.; Liu, C. C. Immunopathogenesis of dengue virus infection. *J. Biomed. Sci.* **2001**, *8* (5), 377–388.
(8) Bonner, S. M.; O'Sullivan, M. A. Endothelial cell monolayers as a model system to investigate dengue shock syndrome. *J. Virol. Methods* **1998**, *71* (2), 159–167.
(9) Andrews, B. S.; Theofilopoulos, A. N.; Peters, C. J.; Loskutoff, D. J.; Brandt, W. E.; Dixon, F. J. Replication of Dengue and Junin Viruses in Cultured Rabbit and Human Endothelial Cells. *Infect. Immun.* **1978**, *20* (3), 776–781.
(10) Miccheli, A. T.; Miccheli, A.; Di Clemente, R.; Valerio, M.; Coluccia, P.; Bizzarri, M.; Conti, F. NMR-based metabolic profiling of human hepatoma cells in relation to cell growth by culture media analysis. *Biochim. Biophys. Acta, Gen. Subj.* **2006**, *1760* (11), 1723–1731.
(11) Odunsi, K.; Wollman, R. M.; Ambrosone, C. B.; Hutson, A.; McCann, S. E.; Tammela, J.; Geisler, J. P.; Miller, G.; Sellers, T.; Cliby, W.; Qian, F.; Keitz, B.; Intengan, M.; Lele, S.; Alderfer, J. L. Detection of epithelial ovarian cancer using H-1-NMR-based metabonomics. *Int. J. Cancer* **2005**, *113* (5), 782–788.
(12) Mortishire-Smith, R. J.; Skiles, G. L.; Lawrence, J. W.; Spence, S.; Nicholls, A. W.; Johnson, B. A.; Nicholson, J. K. Use of metabonomics to identify impaired fatty acid metabolism as the mechanism of a drug-induced toxicity. *Chem. Res. Toxicol.* **2004**, *17* (2), 165–173.
(13) Dettmer, K.; Aronov, P. A.; Hammock, B. D. Mass spectrometry-based metabolomics. *Mass Spectrom. Rev.* **2007**, *26* (1), 51–78.
(14) Williams, R. E.; Lenz, E. M.; Lowden, J. S.; Rantalainen, M.; Wilson, I. D. The metabonomics of aging and development in the rat: an investigation into the effect of age on the profile of endogenous metabolites in the urine of male rats using H-1 NMR and HPLC-TOF MS. *Mol. BioSyst.* **2005**, *1* (2), 166–175.
(15) Lenz, E. M.; Bright, J.; Knight, R.; Westwood, F. R.; Davies, D.; Major, H.; Wilson, I. D. Metabonomics with H-1-NMR spectroscopy and liquid chromatography-mass spectrometry applied to the investigation of metabolic changes caused by gentamicin-induced nephrotoxicity in the rat. *Biomarkers* **2005**, *10* (2−3), 173–187.
(16) Product Information Sheet for ATCC CRL-2922TM. In Manassas, VA, USA.
(17) Fundamental Techniques in Cell Culture. . A Laboratory Handbook. Chapter 12: Cell Culture Protocols. http://www.sigmaaldrich.com/life-science/cell-culture/learning-center/ecacc-handbook/cell-culture-techniques-12.html (accessed 5 Mar 2010).
(18) Kell, D. B.; Brown, M.; Davey, H. M.; Dunn, W. B.; Spasic, I.; Oliver, S. G. Metabolic footprinting and systems biology: The medium is the message. *Nat. Rev. Microbiol.* **2005**, *3* (7), 557–565.
(19) Mapelli, V.; Olsson, L.; Nielsen, J. Metabolic footprinting in microbiology: methods and applications in functional genomics and biotechnology. *Trends Biotechnol.* **2008**, *26* (9), 490–497.
(20) Villas-Boäs, S.; Roessner, U.; Hansen, A. E. M.; Smedsgaard, J.; Nielsen, J. *Metabolome Analysis-An Introduction*; John wiley and sons: Hoboken, NJ, 2007.
(21) Wishart, D. S.; Knox, C.; Guo, A. C.; Eisner, R.; Young, N.; Gautam, B.; Hau, D. D.; Psychogios, N.; Dong, E.; Bouatra, S.; Mandal, R.; Sinelnikov, I.; Xia, J. G.; Jia, L.; Cruz, J. A.; Lim, E.; Sobsey, C. A.; Shrivastava, S.; Huang, P.; Liu, P.; Fang, L.; Peng, J.; Fradette, R.; Cheng, D.; Tzur, D.; Clements, M.; Lewis, A.; De Souza, A.; Zuniga, A.; Dawe, M.; Xiong, Y. P.; Clive, D.; Greiner, R.; Nazyrova, A.; Shaykhutdinov, R.; Li, L.; Vogel, H. J.; Forsythe, I. HMDB: a knowledgebase for the human metabolome. *Nucleic Acids Res.* **2009**, *37*, D603–D610.
(22) Wishart, D. S.; Tzur, D.; Knox, C.; Eisner, R.; Guo, A. C.; Young, N.; Cheng, D.; Jewell, K.; Arndt, D.; Sawhney, S.; Fung, C.; Nikolai, L.; Lewis, M.; Coutouly, M. A.; Forsythe, I.; Tang, P.; Shrivastava, S.; Jeroncic, K.; Stothard, P.; Amegbey, G.; Block, D.; Hau, D. D.; Wagner, J.; Miniaci, J.; Clements, M.; Gebremedhin, M.; Guo, N.; Zhang, Y.; Duggan, G. E.; MacInnis, G. D.; Weljie, A. M.; Dowlatabadi, R.; Bamforth, F.; Clive, D.; Greiner, R.; Li, L.; Marrie, T.; Sykes, B. D.; Vogel, H. J.; Querengesser, L. HMDB: the human metabolome database. *Nucleic Acids Res.* **2007**, *35*, D521–D526.
(23) Ulrich, E. L.; Akutsu, H.; Doreleijers, J. F.; Harano, Y.; Ioannidis, Y. E.; Lin, J.; Livny, M.; Mading, S.; Maziuk, D.; Miller, Z.; Nakatani, E.; Schulte, C. F.; Tolmie, D. E.; Wenger, R. K.; Yao, H. Y.; Markley, J. L. BioMagResBank. *Nucleic Acids Res.* **2008**, *36*, D402–D408.
(24) Smith, C. A.; O'Maille, G.; Want, E. J.; Qin, C.; Trauger, S. A.; Brandon, T. R.; Custodio, D. E.; Abagyan, R.; Siuzdak, G. METLIN - A metabolite mass spectral database. *Ther. Drug Monit.* **2005**, *27* (6), 747–751.
(25) Nicholson, J. K.; Foxall, P. J. D.; Spraul, M.; Farrant, R. D.; Lindon, J. C. 750-MHz H-1 and H-1-C-13 NMR-Spectroscopy of Human Blood-Plasma. *Anal. Chem.* **1995**, *67* (5), 793–811.
(26) Teng, Q.; Huang, W. L.; Collette, T. W.; Ekman, D. R.; Tan, C. A direct cell quenching method for cell-culture based metabolomics. *Metabolomics* **2009**, *5* (2), 199–208.
(27) Brooks, J. B.; Kuno, G.; Craven, R. B.; Alley, C. C.; Wycoff, B. J. Studies of metabolic changes in cell cultures infected with four serotypes of dengue fever viruses by frequency-pulsed electron capture gas-liquid chromatography. *J. Chromatogr.* **1983**, (276), 279–288.
(28) Lei, H.-Y.; Huang, K.-J.; Lin, Y.-S.; Yeh, T.-M.; Liu, H.-S.; Liu, C.-C. Immunopathogenesis of Dengue Hemorrhagic Fever. *Am. J. Infect. Dis.* **2008**, *4* (2), 1–9.
(29) Moran, A. L.; Scrimgeour, K. G.; Horton, H. R.; Ochs, S. R.; Rawn, J. D. *Biochemistry*, 2nd ed.; Neil Patterson: Englewood Cliffs, NJ, 1994.
(30) Garrett, R. H.; Grisham, C. M., *Biochemistry*; Brooks/Cole, Thomas Learning, Inc.: Belmont, CA, 2005.
(31) Knox, C.; Young, N.; Wishart, D. http://hmdb.ca/metabolites/HMDB00267 (accessed 12 July 2010).
(32) Knox, C.; Young, N.; Wishart, D. http://hmdb.ca/metabolites/HMDB00491 (accessed 6 October 2010).

PR100727M